

Tin Powder Preparation by Electrodeposition of Tin Chloride in a Choline Chloride-Ethylene Glycol Deep Eutectic Solvent

Rudi Subagja*, Aga Ridhova, Bunga Rani Elvira, Ari Yustisia Akbar, Nurhayati Indah Ciptasari, Iwan Setiawan, Bintang Adjiantoro, Wahyu Mayangsari, Yudi Nugraha Thaha, Agus Budi Prasetyo and Januar Irawan
Research Center for Metallurgy, National Research and Innovation Agency, KST. B.J. Habibie building 720, Tangerang Selatan, Banten, Indonesia

* Corresponding author. E-mail: rudi001@brin.go.id

DOI: 10.14416/j.asep.2025.05.001

Received: 1 November 2024; Revised: 19 December 2024; Accepted: 7 February 2025; Published online: 7 May 2025

© 2025 King Mongkut's University of Technology North Bangkok. All Rights Reserved.

Abstract

Tin powder is widely used in industry as a raw material for making various products. In this study, the tin powder is prepared by electrodeposition of a mixed solution of tin chloride with a deep eutectic solvent as the electrolyte, to investigate the impact of electrodeposition variables on the current efficiency and the tin morphology produced at the surface of the stainless steel 316 cathode. A cyclic voltammetry test was applied to observe the characteristics of the electrolyte solutions, and the electrodeposition experiment was applied to investigate the impact of technological variables on current efficiency and tin morphology formed at the stainless 316 cathode surface. Experimental findings show that in the cyclic voltammetry test, increasing the tin amounts in electrolyte solutions from 5 to 30 g L⁻¹ increased the cathodic peak current, and the higher tin amount creates a higher current density. While in the electrodeposition process, the cathode current efficiency increased when the electrodeposition current was raised from 2.5 to 6.88 A dm⁻² or the tin amounts in the electrolyte solution were raised from 5 to 10 g L⁻¹. Additionally, smaller tin particles were produced at a higher current density, lower temperature, and lower tin amount.

Keywords: Current efficiency, Cyclic voltammetry, Deep eutectic solvent, Electrodeposition, Morphology, Tin

1 Introduction

The tin powder is widely used in industry as a raw material for making various products such as a solder paste [1], lithium batteries [2], [3], low-temperature superconductor Nb₃Sn [4], Cu-Sn powder alloys [5], Sn-Sb-Cu Babbitt for sliding bearings and liners bearing alloy [6], Mg-Sn alloys [7], Ti-Mn alloy for biocompatible material [8], and carbon fiber-reinforced plastics as coating material [9].

Tin metal powders are generally prepared by various methods such as solid-state reduction, atomization, chemical reduction, and electrochemical deposition [10]. However, solid-state reduction and atomization methods have some drawbacks. Solid-state reduction produces tin powder with low purity and high energy cost [11], while the atomization process has a problem forming satellite particles and

is rather challenging to produce nanoparticles [12]. Even though additional methods, such as ball milling, were employed, they remained less efficient due to the ductile physical properties of tin metal. On the other hand, electrochemical deposition is an inexpensive and versatile technique to produce fine and high-purity tin powder in a one-stage process [13]. Various morphology, size, and chemical composition can be produced by adjusting temperature, electrolyte composition, reduction potential, and reaction time.

Acidic electrolyte solutions are commonly utilized in the tin electrodeposition by standard methodologies. Examples of these electrolytes are sulfuric, citric, boric, hydrochloric, and methane-sulfonic acid [14], [15]. The formation of hydrogen gas, which might reduce the electrodeposition's current efficiency, was the issue with the traditional method [16]. In addition, acidic inorganic compounds

are typically expensive, unbiodegradable, and environmentally hazardous. Therefore, it is critical to find alternative electrolytes that can address these issues.

In recent years, deep eutectic solvent (DES) has been developed as an alternative solvent in a number of industrial sectors due to the growing need for more ecologically friendly operations [17]. In the lignocellulose biorefinery process, DES is utilized as a solvent to provide a green solution to the recalibrated issue [18]. In the metallurgy process, DES is employed as an electrolyte in electrodeposition, metal extraction, or recycling processes [19]. DES is a liquid consisting of hydrogen bond acceptors and donors [20]. DESs offer some advantages, such as high conductivity, wide operation temperature ranges, and nontoxicity, making them suitable for metal alloy deposition. Choline chloride-based DES has been widely used in the metallurgy field and is available in many combinations, such as ethylene glycol, urea, oxalic acid, and malonic acid. The combination of choline chloride and ethylene glycol is preferable due to its properties, which have the lowest viscosity and highest electrical conductivity, broad electrochemical window, biodegradable, and environmentally friendly [20], [21]. Therefore, it is selected in this current research as an electrolyte solution in the tin powder preparation using the electrodeposition method.

DES was employed in several research projects to precipitate metal from the solution. Silver microparticles can be produced electrochemically in DES electrolytes, as demonstrated by silver electrodeposition on the platinum electrode in a DES containing choline chloride-ethylene glycol and choline chloride-urea [22]. It was also applied in a sequential separation process to extract lithium, nickel, and cobalt from lithium-containing batteries with recovery efficiencies of 99.9%, 96.5%, and 98.1% serially [23]. Moreover, antimony powder with a specific form and size was prepared from the mixed solution of antimony chloride by adjusting some electrodeposition parameters in the electrodeposition process using DES containing choline chloride-ethylene glycol [24]. Not only antimony but also good-quality copper, indium, nanocrystalline Fe-Cr alloys, and zinc were produced by this process [21], [25]–[28]. Furthermore, some metallic substrates were used in electrochemical deposition using DES containing choline chloride-ethylene glycol. Indium can be successfully deposited on tungsten and copper electrodes [25], and zinc and zinc–tin alloy coating

were successfully plated on a 1020 carbon steel substrate [27].

Process variables, including current density, temperature, the amount of metal in the electrolyte, the pH of the electrolyte solutions, and electrode materials, could affect the shape of the deposited material that was generated on the cathode surface during the electrodeposition process [29], [30]. However, there is a lack of research on producing fine tin powder, primarily on the effects of technological process variables on the current efficiency and the morphology of tin deposited on the stainless 316 (SS 316) cathode. Therefore, the research aims to investigate the impact of the electrodeposition process variables on the current efficiency and morphology of tin deposited on the SS 316 cathode. This research highlighted the influence of process parameters for the tin electrodeposition, particularly the effect of temperature, tin concentration, and current density on the tin powder morphology, which is essential to designing tin powder-based products for various applications.

2 Materials and Method

2.1 Materials

The tin metal plate with a purity of 99.9 % and the SS 316 plate were respectively used as raw material for the anode and cathode in the electrodeposition experiment. The size of the tin plate was 1 cm thick, 2 cm wide, and 2 cm high. The size of the SS 316 plate was 2 mm thick, 2 cm wide, and 2 cm high. Before the experiment, the surface of the tin plate and SS 316 plate were polished, then washed with demineralized water and dried.

The chemicals used for the experiment were from Merck, i.e., choline chloride, ethylene glycol, and tin chloride dihydrate.

2.2 Method

Figure 1 shows the flow chart for the experiment. The electrolyte solution was prepared by mixing 1 molar choline chloride and 2 molar ethylene glycols in a beaker glass until colorless and homogenous electrolyte solutions were achieved. After that, a certain concentration of tin chloride was added to the mixed choline chloride-ethylene glycol.

This study involved two experiments. The voltammetry test was the first to characterize the

electrolyte solution, and the electrodeposition test was the second to investigate the impact of the electrodeposition process variables, such as temperature, the tin concentration in the electrolyte solution, and current density on the shape of the tin powder produced at the SS 316 cathode surface and the current efficiency. All electrolytes used in this electrodeposition study were DESs containing choline chloride and ethylene glycol with a molar ratio of 1:2.

The experiment used Scanning Electron Microscope (SEM) and Atomic Force Microscope (AFM) to observe the morphology of the tin deposit formed at the SS 316 cathode surface.

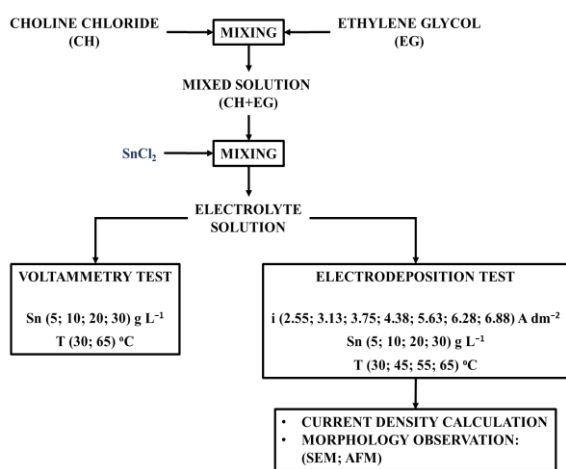


Figure 1: Flowchart for experiment.

3 Result and Discussion

3.1 Cyclic voltammetry of tin chloride in DES of choline chloride-ethylene glycol system

Referring to Bard AJ, cyclic voltammetry could be used to investigate the impact of electrolyte solutions and temperature on electron transfer during the electrodeposition process [31]. In this experiment, three conventional electrode systems were used in the Auto lab PGSTAT 302 N's cyclic voltammetry experiment to characterize electrolyte solutions. These electrodes included a working electrode made of 2 mm diameter of SS 316 wire, a counter electrode made of 2 mm diameter of platinum wire, and an Ag/AgCl electrode with KCl 3 mol/L serving as the reference electrode. These three electrodes were dipped in electrolyte solution in glass containers that contained tin from 5 to 30 g L⁻¹ and DES. The cyclic voltammetry test of the electrolyte solution was

conducted at 30 °C with a scanning rate from 20 to 40 (mV s⁻¹).

Figure 2 represents a cyclic voltammetry curve of the electrolyte solution of mixed tin chloride and DES with a tin concentration of 0.1 g L⁻¹ at a temperature of 30 °C for scan rates of 20 (black line), 30 (red line), and 40 mV s⁻¹ (blue line). This figure illustrates that the beginning of tin reduction occurs at a potential of -0.47 V, and the cathodic peak was observed at approximately -0.69 V, which is in good agreement with the experimental data observed by Rosoiu *et al.*, during the electrodeposition of ternary Sn-Cu-Ni alloys [32]. Anodic peak potential was observed at approximately -0.38 V, signifying the dissolution of Sn to Sn²⁺. This is consistent with the findings of Vieira *et al.*, during the electrodeposition of tin, bismuth, and tin-bismuth alloy from chlorometalate salts in DESs [33] and oxidation of Sn²⁺ to Sn⁴⁺ at the potential of around 0.01 volt.

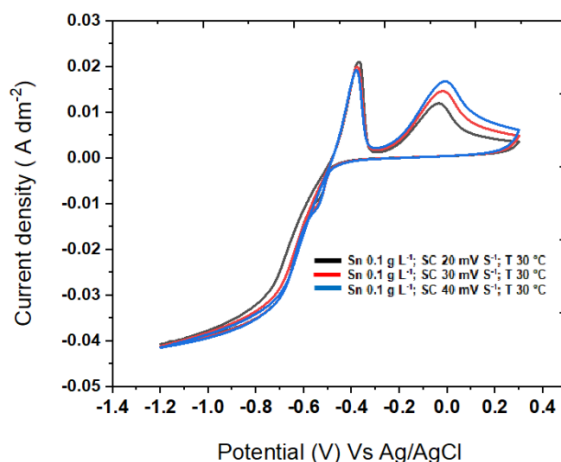


Figure 2: Voltammogram of electrolyte solution with Sn 0.1 gL⁻¹ at temperature 30 °C, scan rate 40 mV s⁻¹ (blue line); 30 mV s⁻¹ (red line); and 20 mV s⁻¹ (black line).

3.1.1 Cathodic sweep voltammetry at a variety of Sn amounts

The cathodic sweep voltammetry test at various tin amounts was carried out on electrolyte solutions containing tin 5 to 30 g L⁻¹ with a scanning rate of 40 mV s⁻¹ at 30 °C. The result in Figure 3 shows that the increase of the tin amount in the electrolyte solution causes the tin reduction potential to shift towards a positive potential, and the solutions with tin amounts of 30 g L⁻¹ have a higher cathodic peak current than

those with a lower tin amount. The higher tin-amount electrolyte provides a higher electron transfer rate and raises the current density at the cathode surface. This experiment result indicates that the increase of tin amount in the electrolyte solution improves the supplement of the ions during the cathodic discharge process [34] and encourages the reduction of Sn^{2+} to metallic tin.

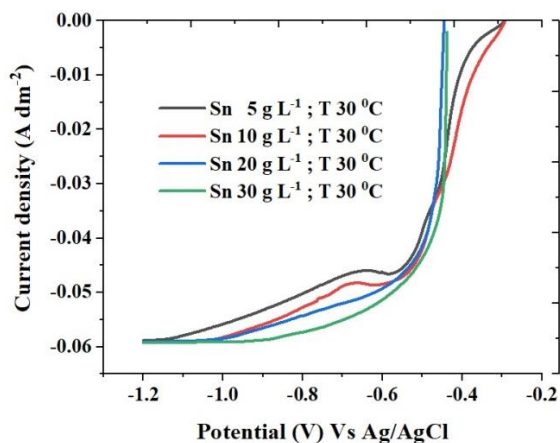


Figure 3: The cathodic sweep voltammetry of electrolyte solutions with various tin amounts at a scanning rate of 40 mV s^{-1} and temperatures of $30 \text{ }^\circ\text{C}$.

3.1.2 Cathodic sweep voltammetry at various electrolyte temperatures

The cathodic sweep voltammetry was conducted on an electrolyte solution containing 10 and 30 g L^{-1} of tin in DES. It was carried out towards a negative potential with a scan rate of 40 mV s^{-1} at $30 \text{ }^\circ\text{C}$ and $65 \text{ }^\circ\text{C}$. We choose this temperature condition to make it suitable for the condition of the electrodeposition experiment. As it is known that temperature plays an important role in the electrodeposition process, increasing temperature can increase solution conductivity and decrease electrolyte solution viscosity [35]. High conductivity causes low energy consumption, while low viscosity causes better ion mobility. At temperatures above $65 \text{ }^\circ\text{C}$, it is possible that excessive evaporation of electrolyte solution will occur.

The results of an experiment in Figure 4 show that raising electrolyte temperatures from 30 to $65 \text{ }^\circ\text{C}$ causes the tin reduction potential curves to shift to a more positive potential and create a higher current density. This phenomenon might be triggered by the increase in the electrolyte temperature, which reduced the electrolyte solution's viscosities, created a more

efficient mass transfer rate, increased electrical conductivities, and raised cathodic peak current. The same tendency was observed by Cao *et al.*, during the voltammetry study of SnCl_2 solution in the choline chloride-urea DES system, using tungsten as the electrode material at temperatures of 50 – $80 \text{ }^\circ\text{C}$, which shows the reduction peak potential of Sn ion shifted to a more positive value and cathodic peak current increases as the temperature increased [36]. Jiacheng *et al.*, studied the effect of temperature on peak current density using cyclic voltammetry of a mixed electrolyte solution of DES containing tin chloride, silver sulfate, and copper chloride, which showed the peak current density rose when the temperature was increased from room temperature to $80 \text{ }^\circ\text{C}$ [37]. Also Wang *et al.*, who prepared a nanocrystalline Fe-Cr alloy coating by electrodeposition in DES, which shows the reduction current density increased as the electrolyte temperature increased [28].

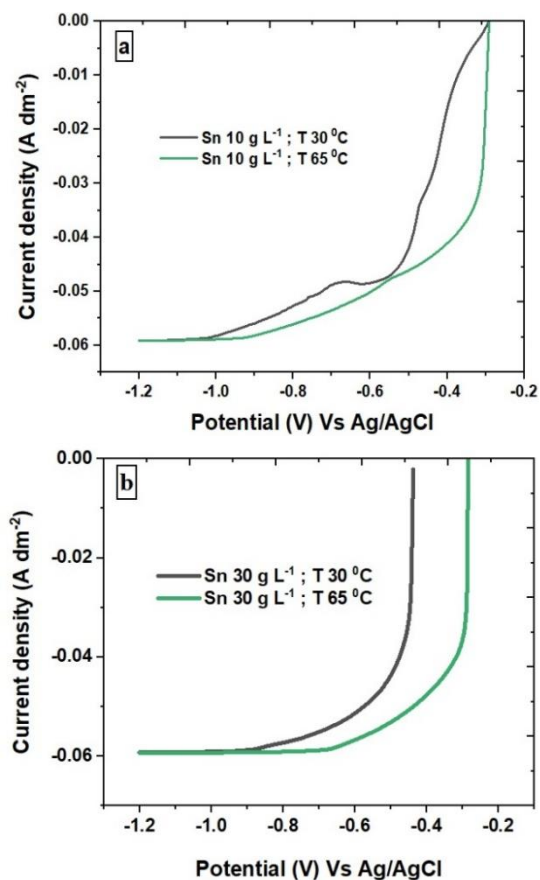
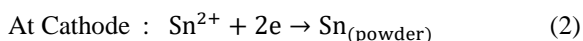
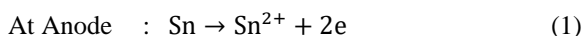


Figure 4: The cathodic sweep voltammetry of electrolyte solutions with varying amounts of tin: (a) 10 g L^{-1} ; (b) 30 g L^{-1} at $30 \text{ }^\circ\text{C}$ and $65 \text{ }^\circ\text{C}$.

3.2 Impact of electrodeposition variables on current efficiency

In the electrodeposition experiment, the electrodeposition cell was filled with electrolyte solutions that contained tin chloride and DES. The tin and SS 316 plates were immersed in the electrolyte solution of the electrodeposition cell. The SS 316 serves as a cathode, and the tin plate serves as the anode. The distance between the tin metal anode and the SS 316 cathode was 3 cm. Direct current flowed from the rectifier into the electrodeposition cell through these two electrodes at a specific current density. As a result of the existence of a direct electric current, the tin ions dissolve from the tin anode following reaction equation 1, and then at the cathode area, the tin ions are reduced to tin metal powder following reaction Equation (2).



The current efficiency is calculated by Equation (3), and the W_T in Equation (3) is calculated by Equation (4),

$$E = (W_A/W_T) \times 100\% \quad (3)$$

$$W_T = (M_{Sn} \times I \times t)/(NF) \quad (4)$$

where current efficiency is symbolized by E; W_A is the actual mass of tin powder created on the surface of SS 316 cathode; W_T is the theoretical tin weight determined applying Faraday's law; M_{Sn} for the weight of tin atomic (118 g/mole); I symbolize for current (ampere); t for time (seconds); N number of movable electrons per atom tin, and F for Faraday constant (96.487 Coulomb/mole).

3.2.1 Impact of applied electrodeposition current

The impact of the applied electrodeposition current on the cathodic current efficiency was observed in an electrolyte solution containing tin of 20 g L⁻¹ in DES at a temperature of 30 °C. The experimental results in Figure 5 show that increasing the applied electrodeposition current from 2.5 to 6.88 A dm⁻² leads to an increase in the current efficiency from 75% to 95.5% due to the anodic surface to bulk solution tin amount differences rising with increased applied

electrodeposition current, promoting the transfer of tin ion metal from the anodic surface to the bulk solution. Concurrently, the cathodic over potential rises with the increase of applied electrodeposition current, stimulating the tin ion discharge and reduction rate at the surface of the cathode and increasing the current efficiency [22].

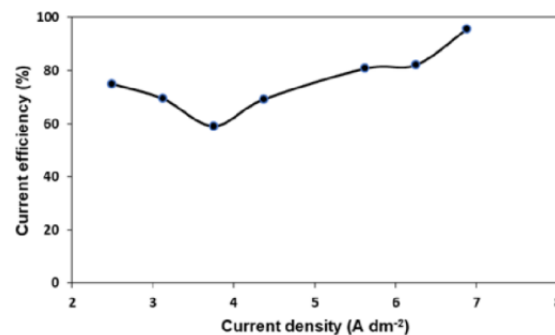


Figure 5: Impact of applied electrodeposition current on current efficiency at a temperature of 30 °C.

3.2.2 Impact of Sn amount in electrolyte solution

The impact of a tin amount in electrolyte solutions on the cathodic current efficiency of the electrodeposition process was observed in the electrolyte solution that has a tin amount of 5 to 30 g L⁻¹ in DES, a temperature of 30 °C, and an applied current density of 5.6 A dm⁻². This current density was chosen because it produced more small-size tin powder particles; approximately 33.83% of tin powder with a particle size smaller than 270 mesh was produced at this current density, while for other current densities, the amount of tin powder with a particle size smaller than 270 mesh was less than 33.83%. The results of the experiment in Figure 6 show that increasing a tin amount in the electrolyte solutions from 5 to 10 g L⁻¹ increases the current efficiency of electrodeposition from 72.7 to 95.3% due to a high tin amount in electrolyte solutions. This stimulates a large supply of tin ions around the surface of the SS 316 cathode, increases the tin reduction, and peak current, as it is supported with the cathodic sweep voltammetry data presented by Figure 3. It is observed that the current density increases, and the tin reduction potential shift to positive potential as the tin amount in the electrolyte solution increased owing to a large supply of the tin ionic species at the cathode surface. A higher tin amount in the electrolyte solution encourages tin reduction at the cathode surface and increases the current efficiency.

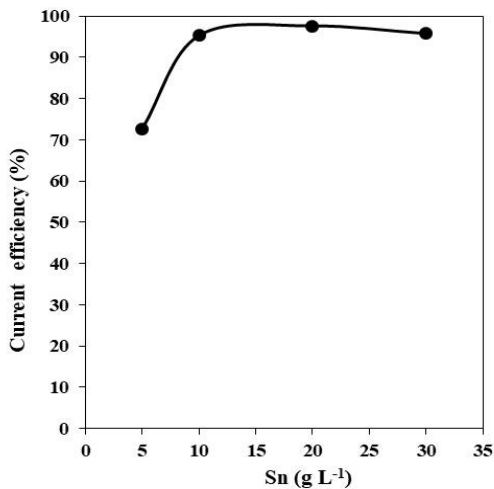


Figure 6: Impact of tin amount in the electrolyte on current efficiency.

3.2.3 Impact of temperature

The electrolyte temperature's impact on the electrodeposition process's current efficiency was investigated in the mixed solution of tin chloride and DES, containing 10 and 30 g L⁻¹ of tin, as an electrolyte solution at a current density of 5.6 dm² for one hour. The experiment's result in Figure 7 shows that in an electrolyte solution with a tin amount of 10 g L⁻¹, increasing electrolyte temperatures from 30 to 65 °C creates an almost constant current efficiency. However, in an electrolyte solution with a tin amount of 30 g L⁻¹, increasing the temperature from 30 to 55 °C increases the current efficiency. This is because the electrolyte solution's conductivity rises, and the viscosity decreases with temperature [35], which increases the amount of Sn (II) ions that are available to reach the surface of the cathode. The diffusion law of Stokes-Einstein states the diffusion coefficient is inversely proportional to viscosity [38]; therefore, increasing in temperature increases the diffusion of ionic tin to the surface of the cathode, which then creates higher current efficiency. This result is in line with the data of cathodic sweep voltammetry at a variety of electrolyte temperatures in Figure 4b, which shows that the increase of electrolyte temperature shifts the tin reduction potential toward the positive potential and increases the current density at the surface of the cathode, which stimulates the tin reduction, and increase current efficiency. Karar *et al.*, noticed a similar tendency during the bismuth electrodeposition, which the cathodic and anodic current density increased with temperature [39].

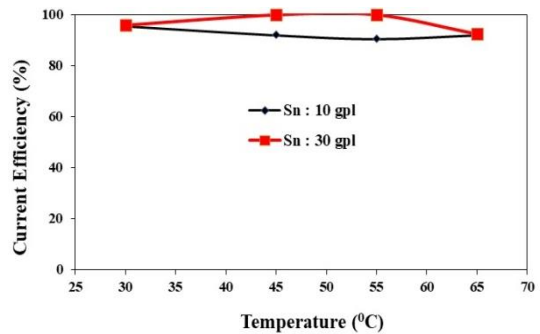


Figure 7: Impact of electrolyte temperature on current efficiency.

3.3 Tin morphology at the surface of the SS 316 cathode

The tin deposited on the surface of the SS 316 cathode was analyzed by SEM and AFM to observe the impact of electrodeposition process variables on the tin morphology formed at the surface of the SS 316 cathode.

3.3.1 Morphology observation by SEM

A small quantity of tin powder metal produced by the electrodeposition process was placed on the sample holder with the help of a double-tape carbon adhesive for SEM analysis. The tin-contained sample holder was then put into the sample chamber room of the SEM for morphology analysis. JEOL JSM - 6390 A type was used in this experiment. Figure 8 shows the tin morphology formed at the surface of the SS 316 cathode, produced by the electrodeposition of the electrolyte solution containing 20 g L⁻¹ of tin in DES at 30 °C for a one-hour electrodeposition process with current densities of 3.1 A dm⁻² and 4.4 A dm⁻². Figure 8 illustrates how increasing the electrodeposition current density from 3.1 A dm⁻² to 4.4 A dm⁻² leads to a change in the morphology of tin powder metal particles from larger to smaller particles. The increase in electrodeposition current led to an increase in the anodic overpotential, which accelerated the tin dissolution rate from the tin anode surface, creating a higher amount of ionic tin near the surface of the anode. This ionic tin should diffuse through the electrolyte solution before it reaches the surface of the cathode side, creating the diffusion-controlled process. At the same time, the cathodic overpotential increases, resulting in a reduction in free energy and critical nucleation radius, which has an impact on accelerating the grain nucleation rate and creating a

smaller tin particle size. The same phenomenon was observed by Zhou *et al.*, during bismuth electrodeposition from an alkaline electrolyte, which shows that the

particle size becomes smaller when the deposition potential increases [40].

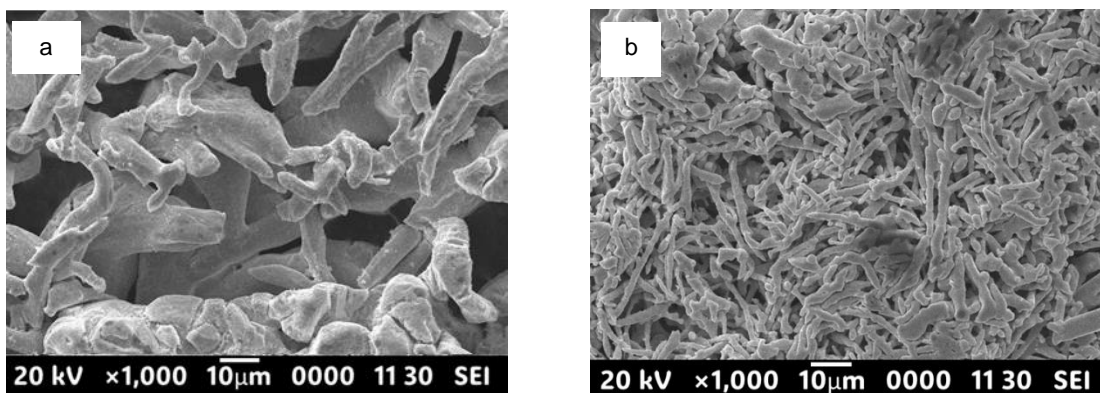


Figure 8: SEM image of the tin powder produced with electrodeposition of 20 g L^{-1} tin electrolyte solution at $30 \text{ }^\circ\text{C}$ for 1 hour, current density: (a) 3.1 A dm^{-2} and (b) 4.4 A dm^{-2} .

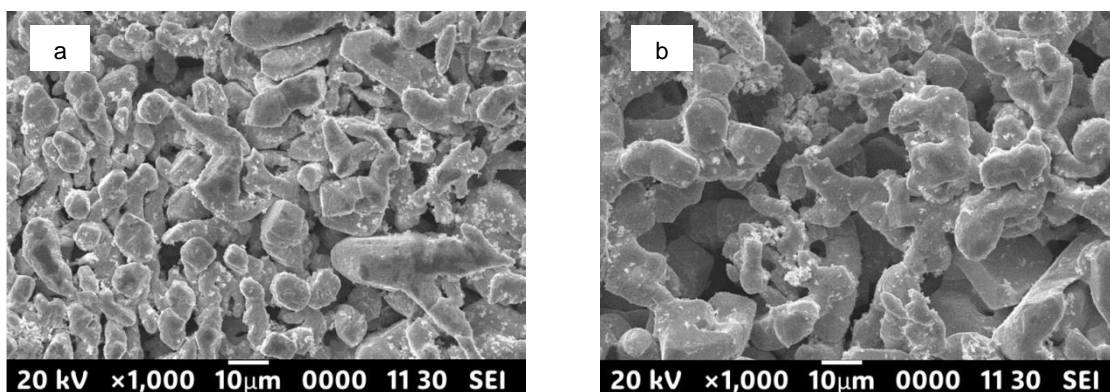


Figure 9: The tin powder morphology produced by one hour electrodeposition process of electrolyte with a tin amount of 10 g L^{-1} in DES and current of 5.6 A dm^{-2} at temperature: (a) $45 \text{ }^\circ\text{C}$; (b) $65 \text{ }^\circ\text{C}$.

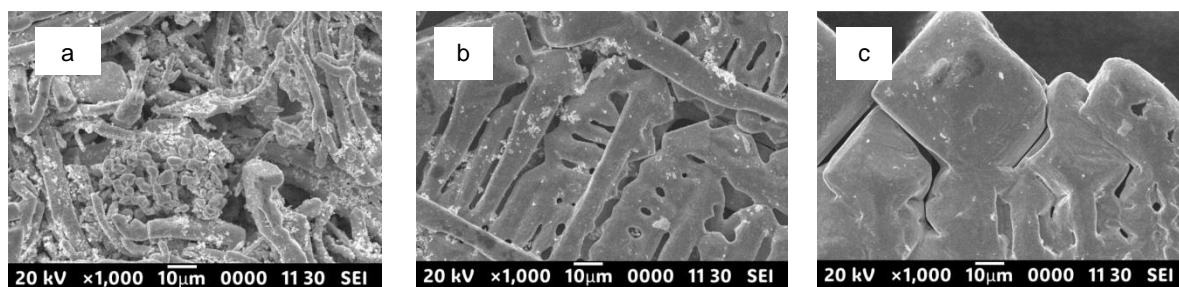


Figure 10: SEM image of tin powder morphology produced at $30 \text{ }^\circ\text{C}$, current of 5.6 A dm^{-2} for 1 h electrodeposition process in an electrolyte solution with Sn amount: (a) 5 g L^{-1} , (b) 10 g L^{-1} , and (c) 30 g L^{-1} .

The tin powder morphology formed at the SS 316 cathode surface also changed when the electrolyte temperature was changed. Figure 9 illustrates the morphology of tin powder produced from the

electrolyte solutions with a tin amount of 10 g L^{-1} in DES at temperatures 45 and $65 \text{ }^\circ\text{C}$ for a one-hour electrodeposition process at a current density of 5.6 A dm^{-2} . The SEM micrograph shows that the tin powder

particle size formed at the SS 316 cathode surface depends on the electrolyte temperature. The tin particle size formed at 65 °C (Figure 9(b)) was larger than that at 45 °C (Figure 9(a)). When the electrolyte temperature was increased, the electrolyte solution viscosity decreased and the electrolyte solution conductivity increased [35], leading to the diffusion process of tin ions being accelerated, the supply of tin ions at the surface of the cathode being faster, increasing the current density and shifts the tin reduction potential towards the positive potential as shown in Figure 4, and therefore increasing the electrodeposition temperature enhanced the tin reduction and enlarges the tin particle size formed at the cathode surface.

The impact of tin amounts in electrolyte solutions on the tin morphology produced at the surface of the SS 316 cathode was observed by SEM. The result in Figure 10 shows that at a temperature of 30 °C and a current density of 5.6 A dm⁻² for a one-hour electrodeposition process, the tin powder particles size produced from the electrolyte solutions with a tin amount of 5 g L⁻¹ (Figure 9(a)) is smaller than that produced in either 10 g L⁻¹ (Figure 10(b)) or 30 g L⁻¹ (Figure 10(c)). This result of SEM observation was supported by the cathodic sweep

voltammetry data in Figure 3, which illustrates that the electrolytes with a higher amount of tin create a higher reduction current density and shift the tin reduction potential towards the positive potential. As a consequence, increasing the tin amounts in the electrolyte solution leads to raising the electron transfer rate and promotes the reduction of Sn(II) at the cathode surface, stimulating the formation of a compact morphology of tin powder particles with larger particle sizes. The same tendency was observed by Kulcsar *et al.*, which shows a larger crystal was produced during the tin electro-refining process in chloride solution as the tin in electrolyte solutions was higher [41], and research by Alexey *et al.*, which shows the average size of the tin in Arc Discharge nanomaterial increased as the tin amount increased [42].

3.3.2 Tin powder morphology observed by Atomic Force Microscope (AFM)

AFM imaging was conducted using the Park NX10 instrument. The tin-coated SS samples were affixed to a 2-cm-diameter sample holder with double-sided tape. The samples were then placed in the instrument, where imaging was performed in non-contact mode using an AC160TS cantilever.

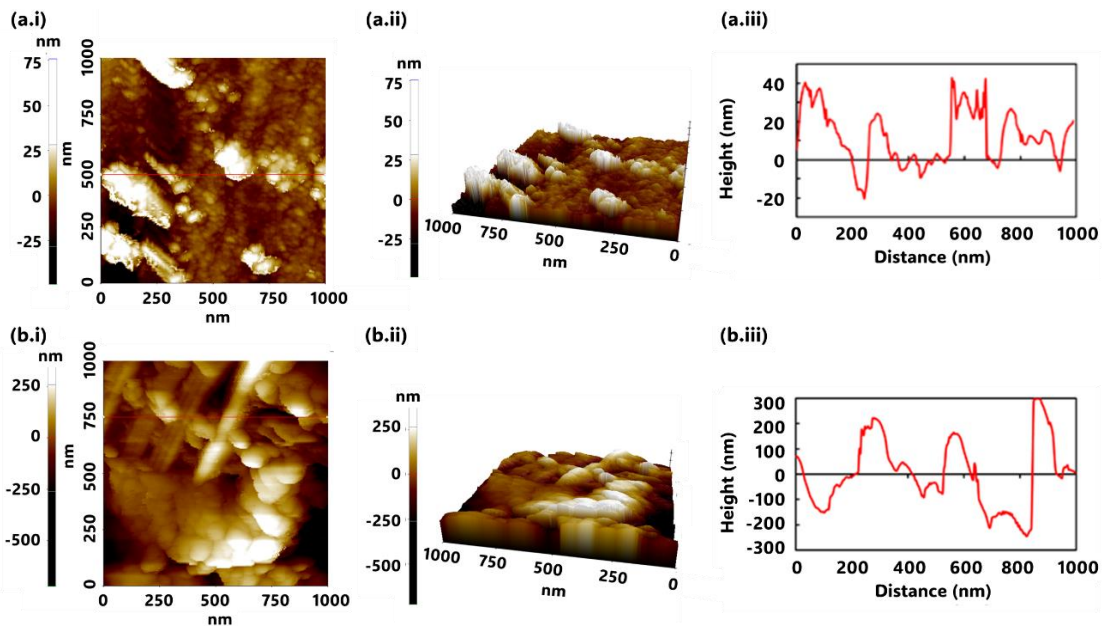


Figure 11: Two-dimensional map (i), three-dimensional AFM images (ii), and section analysis (iii) of tin powder morphology produced from a one-hour electrodeposition process in an electrolyte solution with tin amount of 20 g L⁻¹ in DES at 30°C, current density: (a) 5.6 A dm⁻² and (b) 3.8 A dm⁻².

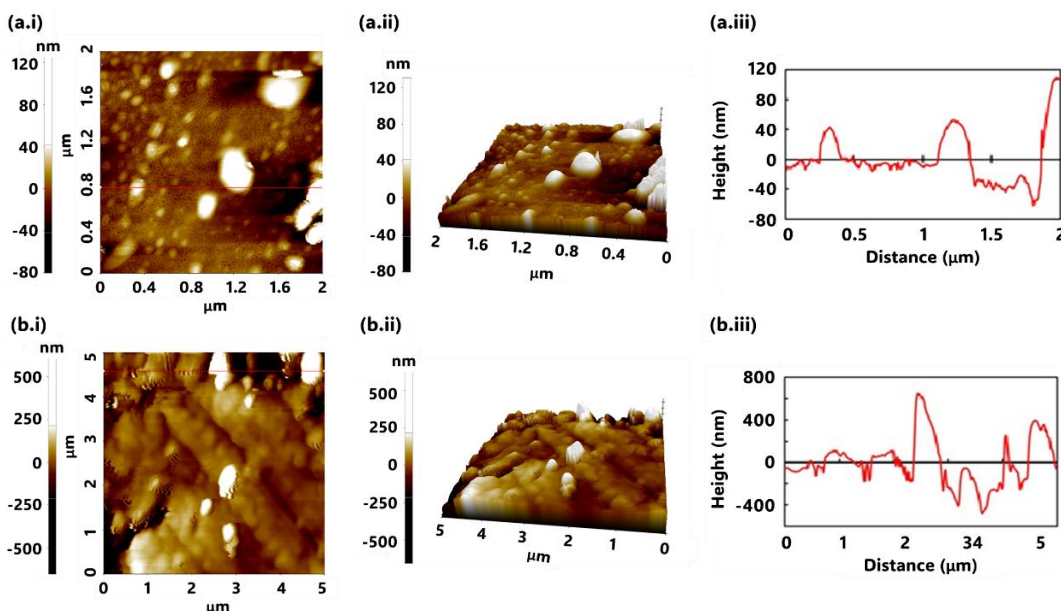


Figure 12: Two-dimensional map (i), three-dimensional AFM images (ii), and section analysis (iii) of tin powder sample obtained by one-hour electrodeposition of electrolyte solution with tin amount: (a) 5 g L^{-1} and (b) 10 g L^{-1} in DES at 30°C , current density 5.6 A dm^{-2} .

Figure 11 shows the two-dimensional map (figures on the left side), three-dimensional AFM images (figures in the middle), and section analysis of the tin powder morphology (figures on the right side) produced from a one-hour electrodeposition process of electrolyte solution containing 20 g L^{-1} tin in DES at 30°C , current density 5.6 A dm^{-2} and 3.8 A dm^{-2} . The roughness analysis reveals that the tin particle height generated at the electrodeposition current density of 5.6 A dm^{-2} (Figure 11(a)) is shorter than the particle height generated at the electrodeposition current density of 3.8 A dm^{-2} (Figure 11(b)). The two-dimensional map and three-dimensional AFM image in Figure 11 also show a tin powder with a smaller crystal structure was generated at an electrodeposition current of 5.6 A dm^{-2} . However, when the electrodeposition current was decreased to 3.8 A dm^{-2} , a larger crystal structure of tin powder was produced. This result of observation by AFM is consistent with the result of observation by SEM in Figure 8, which shows that the morphology of tin powder produced at a higher current density process creates a smaller crystal structure than the tin powder produced at a lower current density.

Figure 12 illustrates the morphology change of the tin metal powder particles produced at different tin amounts in the electrolyte solutions. The figure shows the two-dimensional map, three-dimensional AFM

images, and section analysis of the tin powder morphology produced by a 1-hour electrodeposition process of the tin chloride in the DES, with the tin amount of 5 and 10 g L^{-1} . The electrodeposition experiment was conducted at 30°C with an electrodeposition current density of 5.6 A dm^{-2} . The roughness analysis shows that the height of tin particles produced in the electrolyte solution with a tin amount of 5 g L^{-1} (Figure 12(a)) is shorter than that in 10 g L^{-1} (Figure 12(b)). The figure also shows that the crystal size of tin powder produced in the electrolyte solution with a tin amount of 5 g L^{-1} has a smaller crystal size than that in a tin amount of 10 g L^{-1} . Figure 12 indicates that the morphology of tin particles was affected by the tin amount in the electrolyte solutions; the lower amount of tin in electrolyte solutions creates smaller tin particle size, and the higher amount of tin in electrolyte solution creates a larger particle size. The AFM observation is consistent with the result of observation by SEM in Figure 10, which illustrates that the larger crystal size of tin powder was produced in the electrolyte solution with a higher tin amount.

Figure 13 shows the two-dimensional map, three-dimensional AFM images, and section analysis of a tin-deposited material formed at the surface of the SS 316 cathode produced by a one-hour electrodeposition process of electrolyte solution with a tin amount of 10 g L^{-1} in DES at a current density of

5.6 A dm⁻² and temperature of 30 and 55 °C. The roughness analysis shows that the morphology of tin deposited at 30 °C (Figure 13a) has a shorter height of roughness with a smaller crystal size, while the morphology of tin deposited at 55 °C (Figure 13(b)) has a higher height of roughness and a larger crystal form. This result of observation with AFM is consistent with the result of observation by SEM in Figure 9 which shows that the morphology of tin powder produced by the electrodeposition process at

higher temperatures has a larger crystal form compared to lower temperatures. This is caused by the electrolyte solution viscosity decreasing and the conductivity of the electrolyte solution increasing when the electrolyte temperature was increased [35], leading to diffusion of tin ions, the supply of tin ions at the cathode surface faster, the reduction current density increased and the reduction potential shifts to positive potential as shown by Figure 4, creating a larger crystal size of tin.

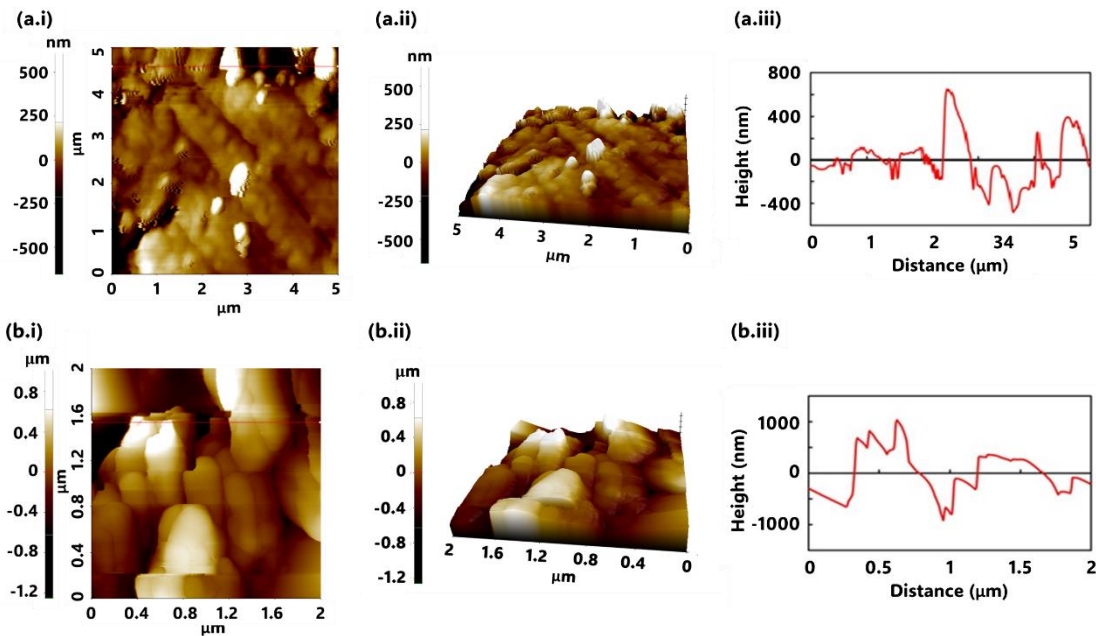


Figure 13: Two-dimensional map (i), three-dimensional AFM images (ii), and section analysis (iii) of a tin powder sample produced by a one-hour electrodeposition process of electrolyte solution with a tin amount of 10 g L⁻¹ in DES at a current density of 5.6 A dm⁻² and temperature of 30 °C (a) and 55 °C (b).

4 Conclusions

Tin powder preparation by electrodeposition of tin chloride has been done in a choline chloride-ethylene glycol deep eutectic solvent. The impact of the electrodeposition process variables on the current efficiency and morphology of tin deposited on SS 316 electrodes has been observed. The result of the experiment leads to the conclusion that electrodeposition current, temperature, and tin amounts in electrolyte solutions affect the current efficiencies and the tin morphology.

Raising the temperatures from 30 to 65 °C decreases the electrolyte solution viscosity and

increases the electrolyte solution conductivity, which accelerates the diffusion of ionic tin from the anode side to the cathode side, increases the tin supply at the cathode surface, creates a higher charge transfer rate at the cathode surface, produces high current efficiency, and creates larger particles of tin metal powder. Raising the tin ion amount in electrolyte solutions from 5 to 30 g L⁻¹ causes abundant ion supply to the cathode surfaces, increases the charge transfer rate at the cathode surface, promotes the reduction of Sn²⁺ at the cathode surface, produces tin powder with a larger particle size, and increases the current efficiency.

Acknowledgments

The authors wish to thank the National Research and Innovation Agency of the Republic of Indonesia for the financial support to conduct these research activities.

Author Contributions

R.S.: design of the experiment, collecting the data, data analysis, writing the manuscript; A.R.: tin morphology observation by AFM; B.R.E.: cyclic voltammetry test; A.Y.A.: cyclic voltammetry test and data analysis; N.I.C.: cyclic voltammetry test; I.S.: design of the electrodeposition experiment; B.A.: tin morphology observation by SEM; W.M.: writing the manuscript; Y.N.T.: data analysis of cyclic voltammetry test result; A.B.P.: preparation of equipment for experiment, J.I.: chemical analysis.

Conflicts of Interest

We disclose that there is no conflict of interest associated with this publication.

References

- [1] A. J. Diaz, D. Ma, A. Zinn, and P. O. Quintero, "Tin nanoparticle-based solder paste for low temperature processing," *Journal of Microelectronics and Electronic Packaging*, vol. 10, no. 4, pp. 129–137, 2013, doi: 10.4071/imaps.386.
- [2] Y. Li, M. Bu, C. Mu, and C. Yang, "Fabricating lithiophilic Sn nanolayer via vacuum evaporation coating for anode-free lithium metal battery," *Materials Letters*, vol. 355, 2024, Art. no. 135449, doi: 10.1016/j.matlet.2023.135449.
- [3] L. Yu, C. Miao, S. Nie, M. Wen, J. Wang, Y. Tan, and W. Xiao, "Feasible preparation of Cu₆Sn₅ alloy thin-film anode materials for lithium-ion batteries from waste printed circuit boards by electrodeposition," *Solid State Ionics*, vol. 364, 2021, Art. no. 115625, doi: 10.1016/j.ssi.2021.115625.
- [4] N. Banno, "Low-temperature superconductors: Nb₃Sn, Nb₃Al, and NbTi," *Superconductivity*, vol. 6, Jun. 2023, Art. no. 100047, doi: 10.1016/j.supcon.2023.100047.
- [5] A. Nassef and M. El-Hadek, "Microstructure and mechanical behavior of hot pressed Cu-Sn powder alloys," *Advances in Materials Science and Engineering*, vol. 2016, no. 1, 2016, Art. no. 9796169, doi: 10.1155/2016/9796169.
- [6] T. E. Abioye, H. Zuhailawati, M. A. I. Azlan, and A. S. Anasyida, "Effects of SiC additions on the microstructure, compressive strength and wear resistance of Sn-Sb-Cu bearing alloy formed via powder metallurgy," *Journal of Materials Research Technology*, vol. 9, no. 6, pp. 13196–13205, 2020, doi: 10.1016/j.jmrt.2020.08.102.
- [7] Özgünn, K. Aslantaş, and A. Ercetin, "Powder metallurgy mg-sn alloys: Production and characterization," *Scientia Iranica*, vol. 27, no. 3B, pp. 1255–1265, 2020, doi: 10.24200/SCI.2019.50212.1578.
- [8] X. Zhou, H. Fang, T. Yuan, and R. Li, "Effect of slight Sn modification on mechanical properties and corrosion behavior of Ti- (2–4 wt%) Mn alloys fabricated via powder metallurgy," *Materials Characterization*, vol. 203, 2023, Art. no. 113068, doi: 10.1016/j.matchar.2023.113068.
- [9] J. Sun, K. Yamanaka, and S. Zhou, "Adhesion mechanism of cold-sprayed Sn coatings on carbon fiber reinforced plastics," *Applied Surface Science*, vol. 579, 2022, Art. no. 151873, doi: 10.1016/j.apsusc.2021.151873.
- [10] E. Bestek, "Powder metallurgy processes and making metal powder," *Materials and Manufacturing Technology*, pp. 2–5, 2020, doi: 10.13140/RG.2.2.21469.84967.
- [11] P. Luo, B. Sun, J. Li, M. Lu, L. Wang, and J. Jiang, "Effect of Antimony (III) on tin recovery by cementation on zinc powder under alkaline conditions," *International Journal of Electrochemical Science*, vol. 14, no. 3, pp. 2621–2630, 2019, doi: 10.20964/2019.03.70.
- [12] Y.W. Kim, K.C. Choi, Y. Chung, E. Choi, and T. Nam, "Microstructure and martensitic transformation characteristics of gas-atomized Ti–Ni–Cu powders," *Journal of Alloys and Compounds*, vol. 577, pp. S227–S231, 2013, doi: 10.1016/j.jallcom.2012.02.041
- [13] G. Rimaszeki, T. Kulcsar, and T. Kekesi, "Investigation and optimization of tin electrorefining in hydrochloric acid solutions", *Journal of Applied Electrochemistry*, vol. 42, no. 8, pp. 573–584, 2012, doi: 10.1007/s10800-012-0433-1.
- [14] J. Lee, J. Kim, B. Chang, H. Kim, and S. Park, "Effects of Ethoxylated α -Naphtholsulfonic acid on tin electroplating at iron electrodes," *Journal of The Electrochemical Society*, vol. 151, no. 5, p. C333, 2004, doi: 10.1149/1.1690289.

- [15] S. H. Son, S. C. Park, J. H. Kim, Y. H. Kim, M. S. Lee, and J. W. Ahn, "Study on the electrorefining of tin in acid solution from electronic waste," *Archives of Metallurgy and Materials*, vol. 60, no. 2, pp. 1217–1220, 2015, doi: 10.1515/amm-2015-0101.
- [16] D. Bilican, J. Fornell, J. Sort, and E. Pellicer, "Electrochemical synthesis of bismuth particles: Tuning particle shape through substrate type within a narrow potential window," *Materials (Basel)*, vol. 10, no. 1, pp. 1–10, 2017, doi: 10.3390/ma10010043.
- [17] L. Tomé, V. Baião, W. Silva, and C. Brett, "Deep eutectic solvents for the production and application of new materials," *Applied Materialstoday*, vol. 10, pp. 30–50, 2018, doi: 10.1016/j.apmt.2017.11.005.
- [18] M. A. Khan, S. Lee, and M. Sriariyanun, "Deep eutectic solvent as a tailor-made chemicals for pretreatment in a lignocellulose biorefinery," *Applied Science and Engineering Progress*, vol. 17, no. 3, pp. 1–4, 2024, doi: 10.14416/j.asep.2024.03.003.
- [19] A. P. Abbott, "Deep eutectic solvents and their application in electrochemistry," *Current Opinion in Green and Sustainable Chemistry*, vol. 36, 2022, Art. no. 100649, doi: 10.1016/j.cogsc.2022.100649.
- [20] B. B. Hansen, S. Spittle, B. Chen, D. Poe, Y. Zhang, J. Klein, A. Horton, L. Adhikari, T. Zelovich, B. Doherty, B. Gurkan, E. Maginn, A. Ragauskas, M. Dadmun, T. Zawodzinski, G. Baker, M. Tuckerman, R. Savinell, and J. Sangoro, "Deep eutectic solvents: A review of fundamentals and applications," *Chemical Reviews*, vol. 121, no. 3, pp. 1232–1285, 2021, doi: 10.1021/acs.chemrev.0c00385.
- [21] A. M. J. Popescu, V. Constantin, M. Olteanu, O. Demidenko, and K. Yanushkevich, "Obtaining and structural characterization of the electrodeposited metallic copper from ionic liquids," *Revista de Chimie*, vol. 62, no. 6, pp. 626–632, 2011.
- [22] N. G. Sousa, C. P. Sousa, O. S. Campos, P. de Lima-Neto, and A. N. Correia, "One-step preparation of silver electrodeposits from non-aqueous solvents," *Journal of Molecular Liquids*, vol. 288, 2019, Art. no. 111091, doi: 10.1016/j.molliq.2019.111091.
- [23] J. Cheng, C. Zheng, K. Xu, Y. Zhu, Y. Song, and C. Jing, "Sequential separation of critical metals from lithium-ion batteries based on deep eutectic solvent and electrodeposition," *Journal of Hazardous Materials*, vol. 465, 2024, Art. no. 133157, doi: 10.1016/j.jhazmat.2023.133157.
- [24] J. Bu, J. Ru, Z. Wang, Y. Hua, C. Xu, Y. Zhang, and Y. Wang, "Controllable preparation of antimony powders by electrodeposition in choline chloride-ethylene glycol," *Advanced Powder Technology*, vol. 30, no. 12, pp. 2859–2867, 2019, doi: 10.1016/j.apt.2019.06.027.
- [25] E. Barrado, S. García, J. A. Rodríguez, and Y. Castrillejo, "Electrodeposition of indium on W and Cu electrodes in the deep eutectic solvent choline chloride-ethylene glycol (1:2)," *Journal of Electroanalytical Chemistry*, vol. 823, pp. 106–120, 2018, doi: 10.1016/j.jelechem.2018.06.004.
- [26] A. Bakkar and V. Neubert, "Recycling of cupola furnace dust: Extraction and electrodeposition of zinc in deep eutectic solvents," *Journal of Alloys and Compounds*, vol. 771, pp. 424–432, 2019, doi: 10.1016/j.jallcom.2018.08.246.
- [27] J. C. Pereira, L. D. Santos, A. A. Alcanfor, H. B. D. Anna, F. X. Feitosa, O. S. Campos, A. N. Correia, P. N. S. Casciano, and P. D. Neto, "Effects of electrodeposition parameters on corrosion resistance of ZnSn coatings on carbon steel obtained from eutectic mixture based on choline chloride and ethylene glycol," *Journal of Alloys and Compounds*, vol. 886, 2021, Art. no. 161159, doi: 10.1016/j.jallcom.2021.161159.
- [28] Z. Wang, T. Wu, J. Ru, Y. Hua, J. Bu, and D. Wang, "Eco-friendly preparation of nanocrystalline Fe-Cr alloy coating by electrodeposition in deep eutectic solvent without any additives for anti-corrosion," *Surface and Coatings Technology*, vol. 406, 2021, Art. no. 126636, doi: 10.1016/j.surfcoat.2020.126636.
- [29] R. Subagja, I. Setiawan, A. R. Rhamdani, and J. Irawan, "Effect of technological parameters on the electrowinning of cobalt from Cobalt(II) chloride solutions," *International Journal of Electrochemical Science*, vol. 17, pp. 1–18, 2022, doi: 10.20964/2022.09.66.
- [30] E. Ciro, A. Dell'era, M. Pasquali, and C. Lupi, "Indium electrowinning study from sulfate aqueous solution using different metal cathodes," *Journal of Environmental Chemical Engineering*, vol. 8, no. 2, 2020, Art. no. 103688, doi: 10.1016/j.jece.2020.103688.

- [31] A. J. Bard, *Electrochemical Methods: Fundamentals and Applications*, 2nd ed. New York: John Wiley & Sons, 2001.
- [32] S. Rosoiu, S. Costovivi, C. Moise, A. Petica, L. Anicai, T. Visan, and M. Enachescu, "Electrodeposition of ternary Sn-Cu-Ni alloys as lead-free solders using deep eutectic solvents," *Electrochimica Acta*, vol. 398, 2021, Art. no. 139339, doi: 10.1016/j.electacta.2021.139339.
- [33] L. Vieira, J. Burt, P. W. Richardson, D. Schloffer, D. Fuchs, A. Moser, P. N. Bartlett, G. Reid, and B. Gollas, "Tin, bismuth, and tin-bismuth alloy electrodeposition from chlorometalate salts in deep eutectic solvents," *ChemistryOpen*, vol. 6, no. 3, pp. 393–401, 2017, doi: 10.1002/open.201700045.
- [34] X. Cao, L. Xu, Y. Shi, Y. Wang, and X. Xue, "Electrochemical behavior and electrodeposition of cobalt from choline chloride-urea deep eutectic solvent," *Electrochimica Acta*, vol. 295, pp. 550–557, 2019, doi: 10.1016/j.electacta.2018.10.163.
- [35] A. Al-Murshedi, H. F. Alesary, and R. Al-Hadrawi, "Thermophysical properties in deep eutectic solvents with/without water," *Journal of Physics: Conference Series*, vol. 1294, no. 5, 2019, doi: 10.1088/1742-6596/1294/5/052041.
- [36] X. Cao, L. Xu, C. Wang, S. Li, D. Wu, Y. Shi, F. Liu, and X. Xue, "Electrochemical behavior and electrodeposition of Sn coating from choline chloride-urea deep eutectic solvents," *Coatings*, vol. 10, no. 12, pp. 1–10, 2020, doi: 10.3390/coatings10121154.
- [37] J. Huang, W. Wang, Q. Xiang, S. Xin, P. Wang, N. Mitsuzaki, and Z. Chen, "Effect of deposition potential on electrodeposition of Sn-Ag-Cu ternary alloy solderable coating in deep eutectic solvent," *Journal of Electroanalytical Chemistry*, vol. 943, 2023, doi: 10.1016/j.jelechem.2023.117613.
- [38] C. C. Miller, "The stokes einstein law for diffusion in solution," in *Proceedings of the Royal Society A: Mathematical, Physical, And Engineering Sciences*, pp. 724–749, 1924.
- [39] Y. Karar, S. Boudinar, A. Kadri, J. C. Leprêtre, N. Benbrahim, and E. Chaïnet, "Ammonium chloride effects on bismuth electrodeposition in a choline chloride-urea deep eutectic solvent," *Electrochimica Acta*, vol. 367, 2021, Art. no. 137481, doi: 10.1016/j.electacta.2020.137481.
- [40] L. Zhou, Y. Dai, H. Zhang, Y. Jia, J. Zhang, and C. Li, "Nucleation and growth of bismuth electrodeposition from alkaline electrolyte," *Bulletin of the Korean Chemical Society*, vol. 33, no. 5, pp. 1541–1546, 2012, doi: 10.5012/bkcs.2012.33.5.1541.
- [41] T. Kulcsar, G. B. Toth, and T. Kekesi, "Complex evaluation and development of electrolytic tin refining in acidic chloride media for processing tin-based scrap from lead-free soldering," *Transactions of the Institutions of Mining and Metallurgy: Section C Mineral Processing and Extractive Metallurgy*, vol. 125, no. 4, pp. 228–237, 2016, doi: 10.1080/03719553.2016.1206693.
- [42] A. V. Zaikovskii, A. A. Iurchenkova, D. V. Kozlachkov, and E. O. Fedorovskaya, "Effects of tin on the morphological and electrochemical properties of arc-discharge nanomaterials," *Journal of the Minerals, Metals & Materials Society*, vol. 73, no. 3, pp. 847–855, 2021, doi: 10.1007/s11837-020-04556-z.